

Short communication

Aqueous phase hydrogenation of furfural to tetrahydrofurfuryl alcohol over Pd/UiO-66

Chunhua Wang^{a,b}, Anjie Wang^{a,b}, Zhiquan Yu^{a,b}, Yao Wang^{a,b}, Zhichao Sun^{a,b}, Victor M. Kogan^c, Ying-Ya Liu^{a,b,*}

^a State Key Laboratory of Fine Chemicals, School of Chemical Engineering, Dalian University of Technology, Dalian 116024, PR China

^b Liaoning Key Laboratory of Petrochemical Technology and Equipment, Dalian University of Technology, Dalian 116012, PR China

^c N. D. Zelinsky Institute of Organic Chemistry, Russian Academy of Sciences, Moscow 119991, Russia

ARTICLE INFO

Keywords:

Pd/UiO-66

Catalyst

Hydrogenation

Furfural

Tetrahydrofurfuryl alcohol

ABSTRACT

A Pd/UiO-66 catalyst was synthesized with well-dispersed Pd nanoparticles. The obtained catalyst was tested in the hydrogenation of furfural to tetrahydrofurfuryl alcohol in various solvents, Water was found to be the most suitable solvent. Pd/UiO-66 exhibited much higher activity than Pd/SiO₂ and Pd/ γ -Al₂O₃, completely converting furfural to tetrahydrofurfuryl alcohol with 100% selectivity under mild conditions. The hydrogenation of C=O moiety in tetrahydrofurfural was rate-determining step. Static adsorption measurement indicated that the adsorption of furfural on UiO-66 was significantly stronger than that on SiO₂ or γ -Al₂O₃, suggesting that the adsorption play an important role in the gas-liquid-solid furfural hydrogenation reaction.

1. Introduction

Biomass and its derivatives have attracted increasing attention in the production of renewable biofuels and value-added compounds due to the environmental concerns [1]. Furfural (FAL) is mainly obtained by acid-catalyzed dehydration of xylan, which mainly exists in the hemicellulose components of lignocellulosic biomass [2]. Because of the rich unsaturated bond in its structure, the catalytic hydrogenation of FAL gives rise to a number of valuable chemicals [3], including furfuryl alcohol (FOL), 2-methyl furan (2-MF), furan, tetrahydrofuran, cyclopentanone (CPO) and tetrahydrofurfuryl alcohol (THFOL), the hydrogenation products depend highly on the catalyst and the reaction conditions [4].

THFOL is a total hydrogenation product, which is widely used as a green solvent in pharmaceutical, industrial and agricultural sectors [3]. In industry, the production of THFOL from FAL involves two consecutive steps: hydrogenation of FAL to afford FOL and further hydrogenation of FOL to THFOL [5]. It is highly desirable to synthesize THFOL from FAL in one step [6,7]. Noble metal catalysts are commonly used in hydrogenation of FAL to THFOL. Pd-based catalyst with specific supports such as carbon [8], Al₂O₃ [9], hydroxyapatite [10], SiO₂ [4], MIL-101(Cr)-NH₂ [11] have shown good catalytic activity, due to the synergies of supports and active metal. Solvent significantly influences the catalyst performance and the product selectivity in the

hydrogenation of FAL [12,13]. When alcohols were used, acetals were produced as the typical byproducts [7,14]. In contrast, water can avoid the formation of acetalization product, but the variation of temperature can influence the product distribution [15,16]. Therefore, developing environmentally-friendly catalyst with high selectivity of THFOL under mild condition is still a challenge [10].

Metal-organic frameworks (MOFs) have shown great promise in heterogeneous catalysis, due to their high surface areas and well-defined porosities [17]. Yin et al. reported a 3 wt% Pd@MIL-101(Cr)-NH₂ could catalyze hydrogenation of FAL to THFOL at 40 °C and 2 MPa H₂ in water. The initial selectivity was close to 100%, but it decreased to 90% in the second run [11]. UiO-66 is one of the considerably stable MOFs, it is built up from [Zr₆O₄(OH)₄(CO₂)₁₂] clusters linked with terephthalate ligand, to obtain a porous cubic architecture [18]. UiO-66 has relatively good chemical stability resistance to water and organic solvents. Recently, Yang et al. prepared a Pd/UiO-66-v (v represents the vinyl functional group on the MOF ligand), which showed high activity in the hydrogenation of FOL, with 99% conversion and 90% selectivity to THFOL at 0.5 MPa H₂, 303 K for 12 h in water [19]. The high performances of UiO-66 supported noble metal catalysts are believed to be associated with the high dispersion of noble metals and favorable surface properties for reactant adsorption [15,16,19].

In this paper, Pd/UiO-66 was prepared by impregnation, and tested in the hydrogenation of FAL, the catalytic performance with compared

* Corresponding author at: School of Chemical Engineering, Dalian University of Technology, West Campus B225, 2 Linggong Road, Dalian 116024, PR China.
E-mail address: yingya.liu@dlut.edu.cn (Y.-Y. Liu).

<https://doi.org/10.1016/j.catcom.2020.106178>

Received 7 July 2020; Received in revised form 25 September 2020; Accepted 2 October 2020

Available online 03 October 2020

1566-7367/ © 2020 Elsevier B.V. All rights reserved.

with Pd/SiO₂ and Pd/ γ -Al₂O₃ catalysts. The effects of solvent, catalyst dosage, temperature, and hydrogen pressure in the reaction were investigated, and the reusability of Pd/UiO-66 was studied as well.

2. Experimental

2.1. Characterization

Powder X-ray diffraction (XRD) data was collected on a Rigaku D/Max-2400 diffractometer with Ni-filtered Cu-K α radiation at 40 kV and 100 mA. The BET specific surface area was calculated from the N₂ adsorption/desorption isotherms which were measured at -196 °C on a Micromeritics Tristar II 3020. The sample was out-gassed under vacuum at 120 °C for 3 h, prior to the adsorption measurement. FT-IR spectrum of UiO-66 (KBr pellet) and Pyridine-adsorbed FT-IR spectrum was recorded on an Equinox 55 FT-IR spectrometer (the detailed experimental procedures was given in Supplementary Information). Elemental analysis was carried out by means of inductively coupled plasma optical emission spectroscopy (ICP-OES) on an Optima 2000DV device. The morphology observation of the sample was carried out on a field-emission scanning electron microscope (FE-SEM) (FEI NOVA NanoSEM 450), and the scanning was performed on the pre-dried sample powder and sputter-coated with a thin layer of gold. Transmission electron microscopy (TEM) images were acquired on Tecnai G2 F30 transmission microscope operated at 300 kV. The sample was suspended in ethanol and deposited on a copper grid prior to observation.

The H₂ chemisorption measurement was carried out using a dynamic pulse method on a Chembet-3000 instrument following the reported procedure [20]. The H₂ uptakes and metal dispersions of the catalysts were calculated based on the equations given by Aramendía et al. [21].

2.2. Catalyst preparation

UiO-66 was synthesized according to the procedure reported by Lillerud and co-workers [18]. The Pd/UiO-66 catalyst was prepared by impregnation. 0.2 g of UiO-66 was dispersed in 5 mL ethanol and sonicated for 30 min at room temperature. 200 μ L aqueous solution of 1.5 wt% PdCl₂ in diluted HCl was dissolved in ethanol, and the Pd-containing solution was added dropwise to the UiO-66 suspension under vigorous stirring. The resulting mixture was stirred at 50 °C for 24 h. Then the solid product was collected by centrifugation and the supernatant was collected for complexometric titration of Pd. The obtained Pd²⁺/UiO-66 was washed three times with ethanol, followed by drying at 120 °C under vacuum for 12 h. Pd²⁺/UiO-66 sample was reduced in a H₂ flow (75 mL/min) at 300 °C for 2 h. After cooling down to room temperature, the resultant catalyst was passivated in a gas flow of 0.5 vol% of O₂ in argon (20 mL/min) for 2 h prior to use.

2.3. Catalytic performance

The catalytic hydrogenation of FAL was carried out in a 75 mL stainless steel Parr autoclave. In a typical experiment, 50 mg of Pd/UiO-66, 100 mg FAL and 9.9 g solvent were added into the autoclave, speed of stirring 750 rpm, and was heated at a specific temperature under H₂ pressure. After reaction, the reactor was cooled to room temperature. The liquid product was centrifuged to separate the catalyst, and the liquid was analyzed by a gas chromatography (Agilent 6890, FID) with a HP-INNOWax capillary column (30 m \times 320 μ m \times 0.5 μ m). The carbon balance of all examined catalysts was in the range of 95 to 98%.

Table 1

The N₂ adsorption and H₂ chemisorption results of UiO-66 and the supported Pd catalysts.

Sample	S _{BET} (m ² .g ⁻¹)	H ₂ uptake (μ mol.g ⁻¹)	D (%)
UiO-66	1342	–	–
Pd/UiO-66	947	6.5	17.9
γ -Al ₂ O ₃	111	–	–
Pd/ γ -Al ₂ O ₃	62	4.4	12.3
SiO ₂	232	–	–
Pd/SiO ₂	126	2.4	6.7

3. Results and discussion

3.1. Catalyst characterization

The XRD patterns of the synthesized UiO-66 and Pd/UiO-66, Pd/ γ -Al₂O₃ and Pd/SiO₂ were shown in Fig. S1. All diffraction peaks of the as-synthesized UiO-66 matched well with the simulated pattern obtained from single crystal X-ray crystal diffraction data [18]. The loading of Pd²⁺ into UiO-66 and subsequent reduction treatment did not markedly change the crystallinity of the parent UiO-66. For γ -Al₂O₃ and SiO₂ the diffraction peaks of each catalyst matched well with those of the corresponding supports, the characteristic XRD peaks of all the Pd crystalline phase were not detectable, probably because the Pd particle size was below the detection limit.

The BET surface area of UiO-66, γ -Al₂O₃ and SiO₂ was 1343, 111 and 232 m²/g, respectively (Table 1). After reduction, the specific surface area of Pd/UiO-66, Pd/ γ -Al₂O₃ and Pd/SiO₂ was decreased moderately to 947, 62 and 126 m²/g, respectively. This observation might be ascribed to the partial occupation of the cavities in supports.

The SEM image of the synthesized UiO-66 is shown in Fig. S2a, the obtained UiO-66 were octahedral crystallites of about 400 nm. The TEM image of Pd/UiO-66 is shown in Fig. S2b. The lattice fringe with an interplanar distance is 0.225 nm, corresponding to the Pd (111) plane. The grain size of Pd particles was in the range of 2–3 nm, suggesting that nanosized Pd particles were highly dispersed in UiO-66.

The metal dispersion was further characterized by H₂ chemisorption, which showed that the H₂ uptake of Pd/UiO-66 was 6.5 μ mol/g, giving the highest dispersion of 17.9 (Table 1). The average particle size calculated based on the dispersion was 6.2 nm, which was larger than that observed on TEM. It is likely that not all the surface metal sites of Pd particles in the pores of UiO-66 were available for H₂ adsorption due to the pore blockage.

Fig. 1 shows the FT-IR spectra of pyridine adsorbed on UiO-66 and Pd/UiO-66 in the region 1400–1700 cm⁻¹. In the spectrum of UiO-66, the bands due to Lewis-bonded pyridine (1455 cm⁻¹), Brønsted-bonded pyridine (1536 cm⁻¹) and the band assigned to pyridine associated with both Brønsted and Lewis acid sites (1498 cm⁻¹), were observed [22]. The Lewis acidity of UiO-66 might originate from the accessible Zr sites [23], as well as from the defects due to the missing organic linkers between Zr₆ clusters [18]. Furthermore, the Brønsted acidity could be attributed to the protonation of the organic linkers in UiO-66. In the spectrum for Pd/UiO-66, the three kinds of bands were all present, without appreciable change of the peak intensity, suggesting that the acidic sites were well preserved.

3.2. Catalytic performance of Pd/UiO-66

In general, the production of THFOL by FAL hydrogenation proceeds mainly via two parallel pathways (Scheme 1): (1) C=O hydrogenation followed by ring hydrogenation; (2) ring hydrogenation followed by C=O hydrogenation. Therefore, FOL and THFAL are the main intermediates.

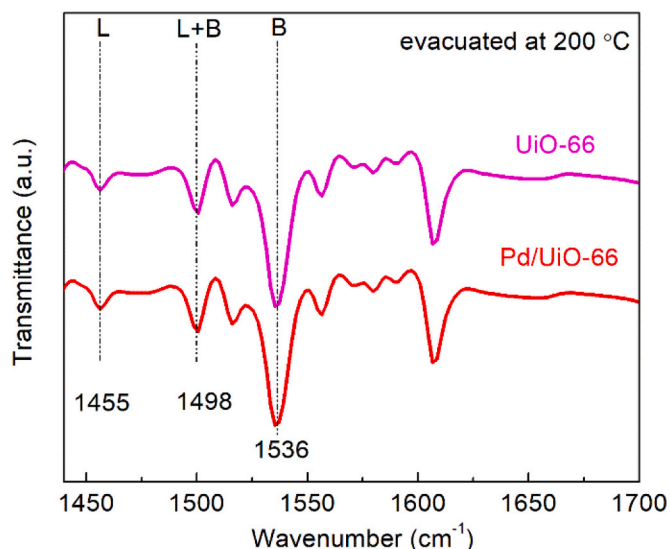


Fig. 1. FT-IR spectra of adsorbed pyridine on UiO-66 and Pd/UiO-66.

3.2.1. Effect of solvent

Solvents have a strong impact on the reaction rates and selectivities in liquid phase [24]. Polar solvents have been reported to be favorable for liquid phase hydrogenation of FAL [25].

To investigate the solvent effects on conversion and product selectivity, protic solvents (water and C₂–C₄ alcohols) and aprotic (toluene) were used in FAL hydrogenation catalyzed by Pd/UiO-66. Table 2 shows that the solvents significantly influenced both FAL conversion and the product distribution. When polar solvents were used, full conversions of FAL were obtained, whereas only 62% FAL was converted in toluene under same conditions. Hu et al. [26], reported that a shielding effect between the conjugated π system in both FAL and toluene could be a major factor that negatively affected the hydrogenation rates of both the furan ring and aldehyde group in FAL.

Alcohol solvents are frequently used for selective hydrogenation of FAL, because the ability of hydrogen donation promotes the hydrogenation rate. As a result, remarkably higher conversion was achieved in an alcohol than in toluene. Nevertheless, when alcohol solvents are used for aldehyde hydrogenation, acetals are usually obtained as the byproducts [14]. The side-reaction of acetalization is correlated with surface acidity of the catalyst support, and might be suppressed over

Table 2
Effect of solvent in FAL hydrogenation catalyzed by Pd/UiO-66.

Solvent	Conversion (%)	Selectivity (%)				
		THFOL	FOL	THFAL	FDA	Others
2-propanol	100	88	1	11	-	-
Water	100	100	-	-	-	-
Ethanol	100	75	5	8	9	3
n-butanol	100	77	7	14	-	2
Toluene	62	41	35	23	-	1

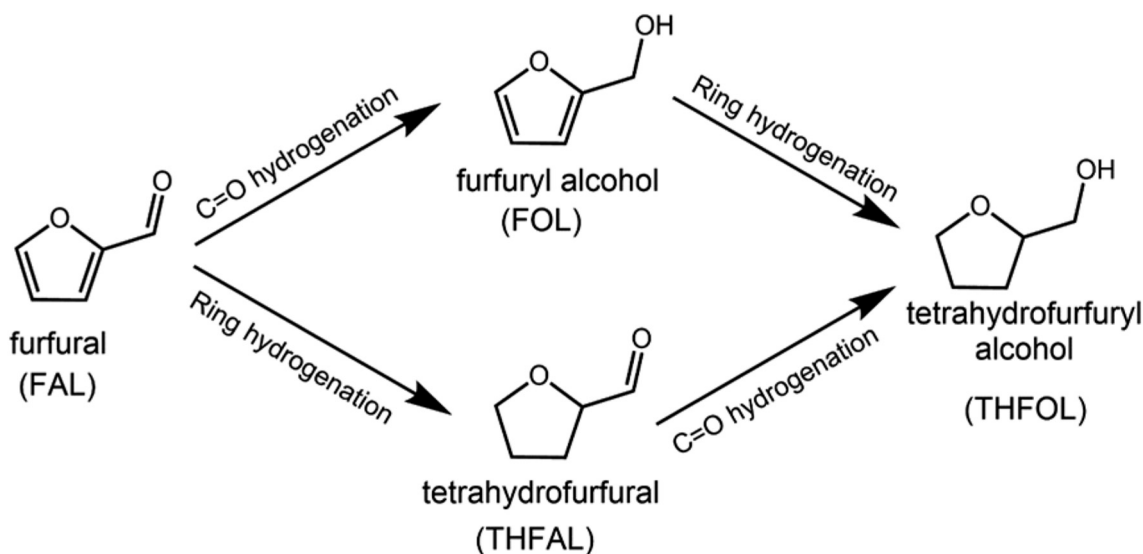
Reaction conditions: 50 mg of 1.2 wt% Pd/UiO-66, 100 mg FAL, 9.9 g solvent, 60 °C, 1.0 MPa, 4 h. THFOL: tetrahydrofurfuryl alcohol, FOL: furfuryl alcohol, THFAL: tetrahydrofurfural, FDA: 2-furaldehyde diethyl acetal.

basic catalyst support [27]. Martin et al. [28], reported that the selectivity towards the undesired acetal decreased with increasing chain length of the alcohol. In the present study, a small amount of 2-furaldehyde diethyl acetal (FDA) was obtained in ethanol, whereas no acetal was detectable in 2-propanol or n-butanol (Table 2). In addition, a literature survey regarding the catalytic performance of different Pd-based catalysts in the hydrogenation of FAL was presented in Table S2, the hydrogenated intermediates (FOL and THFAL) were detected in all the alcohol solvents (Entries 1–7), probably due to lowered hydrogenation efficiency.

Water is also often used as a solvent in the catalytic hydrogenation of FAL. The advantage of water as the solvent is that no acetalization or other side reaction occurs (Entries 8–10, Table S2). From Table 2, it is seen that a perfect FAL full hydrogenation was obtained with 100% FAL conversion and 100% THFOL selectivity. Zhao et al. [29], proposed that water participate directly in the kinetically relevant reaction step and provides an additional channel for hydrogenation of the aldehyde group. Wan et al. [30], tested temporal H₂ uptake profiles in water, C₁–C₄ primary alcohols and aprotic solvents as a function of time by monitoring the pressure drop in the external H₂ reservoir. It was found that water exhibited the highest H₂ uptake rate. In the gas-liquid-solid reaction of FAL hydrogenation over Pd/UiO-66, the dissolution of gaseous H₂ in the solvent is directly linked with the surface coverage of H₂ on the catalyst, which determines the overall reaction rate.

3.2.2. Effect of the support

Table 3 presents the conversion and product selectivity in aqueous phase hydrogenation catalyzed by Pd supported on three different porous materials: UiO-66, γ -Al₂O₃ and SiO₂. The control experiment of



Scheme 1. Reaction network of FAL hydrogenation.

Table 3
FAL hydrogenation over supported Pd catalysts.

Catalyst	Conversion (%)	Selectivity (%)		
		THFOL	FOL	THFAL
UiO-66	-	-	-	-
Pd/UiO-66	100	100	-	-
Pd/ γ -Al ₂ O ₃	100	64	-	36
Pd/SiO ₂	36	10	76	14

Reaction conditions: 50 mg of 1.2 wt% Pd-based catalyst, 100 mg FAL, 9.9 g water, 60 °C, 1.0 MPa, 4 h.

UiO-66 catalyzed hydrogenation of FAL gives no activity, suggesting that the originate UiO-66 did not contribute to the catalytic hydrogenation. FAL conversion increased in the order: Pd/SiO₂ (36%) < Pd/ γ -Al₂O₃ (100%) = Pd/UiO-66 (100%). In addition, the support had a marked influence in the product selectivity. The main product was THFOL for Pd/ γ -Al₂O₃ (64%) and Pd/UiO-66 (100%), whereas FOL was dominant in the product for Pd/SiO₂. Recently, Mironenko et al. [31], reported the effect of the Pd support on the reaction pathway in the aqueous hydrogenation of FAL. They found that a basic MgAl oxide support led to lower performance, and the major products were FOL and THFOL (Entry 9, Table S2). In addition, the adsorption of FAL is essential in determining the hydrogenation rate. Fig. S3 illustrates the variation of FAL adsorbed on each support with time in static adsorption at different FAL concentrations. The adsorption of FAL was fast in the first 30–60 min and then the adsorption gradually reached to saturation. The adsorption capacity decreased in the same order: UiO-66 > γ -Al₂O₃ > SiO₂ at different FAL concentrations. In accordance with the hydrogenation performance of the supported Pd catalysts. The adsorption of FAL on MOFs were reported to be enhanced by the strong interactions between FAL and the MOF support via the C=O bond and their coordinatively unsaturated sites (CUSs) [32,33]. Wan et al. attributed the enhanced adsorption of FAL to the acid sites from the support [30]. Therefore, the presence of Brønsted and Lewis acid sites in UiO-66 (Fig. 1) might be favorable for the adsorption of FAL, thus improving the reaction rate.

Besides, the support affected the formation of hydrogenated intermediates. It implies that the reaction rates of the two parallel pathways might be determined by both active sites and the properties of the supports. For Pd/ γ -Al₂O₃, only THFAL was detected as the intermediate. The absence of FOL might be due to the fast hydrogenation of FOL. For Pd/SiO₂, both THFAL and FOL were present in the hydrogenation product, suggesting that Pd/SiO₂ was much less active in the hydrogenation.

Additionally, the performance of the supported Pd catalyst might be related with the dispersion of Pd nanoparticles. Pd/UiO-66 showed the highest dispersion (Table 1) due to the Pd²⁺ that was anchored on the external surface of UiO-66 via the Pd²⁺ with μ_3 -OH groups on the Zr₆ nodes in the form of Zr-O-Pd bond [34]. So Pd/UiO-66 showed the highest activity and selectivity to THFOL.

3.2.3. Effect of reaction time

In order to identify the possible intermediates, the variation of FAL conversion and product yield with reaction time was investigated (Fig. 2). In the first 5 min, FAL reached 47% conversion with yield of 21% to FOL, 13% to THFOL, and 13% to THFAL, suggesting that FAL hydrogenation to THFOL proceeded in both pathways (Scheme 1). Afterwards, the yield to THFOL increased monotonically up to 100% over time. The yield of FOL rapidly disappeared in 30 min, and no maximum yield of FOL was observed in the time scale, indicating that the subsequent ring hydrogenation of FOL was substantially fast over Pd/UiO-66. On the other hand, the yield of THFAL passed through a maximum at 20 min, and decreased slowly to zero until 250 min. It is

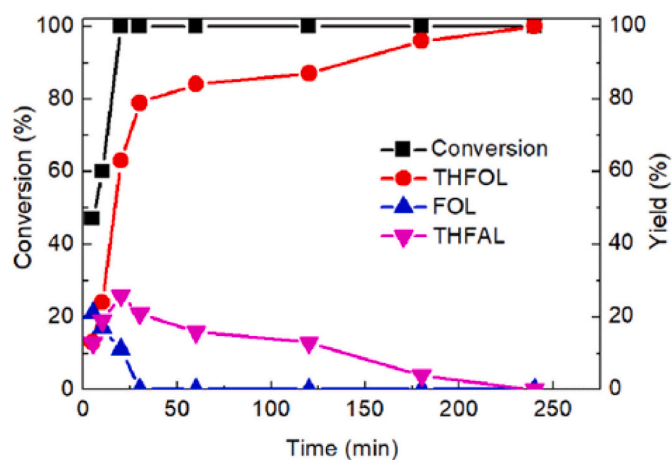


Fig. 2. Variation of conversion and yield with reaction time in FAL hydrogenation catalyzed by Pd/UiO-66. Reaction conditions: 50 mg Pd/UiO-66 catalyst, 100 mg FAL, 9.9 g water, 60 °C, 1.0 MPa.

evident that the hydrogenation started in two parallel pathways, and the ring hydrogenation and C=O hydrogenation took place simultaneously. However, the subsequent C=O hydrogenation of FOL was considerably faster than the subsequent ring hydrogenation of THFAL. The overall rate of the FAL-FOL-THFOL pathway was much faster than that of FAL-THFAL-THFOL, which explained the absence of FOL in the product for the Pd/UiO-66-catalyzed hydrogenation of FAL at full conversion (Table 3). Fig. 2 indicates that the hydrogenation of C=O moiety in THFAL was rate-limiting in the hydrogenation of FAL. Krishna et al. [35], proposed that the hydrogenation ability of the C=O bond was weakened after the C=C bond hydrogenation. To investigate the influence of diffusion limitation, hydrogenation of FAL over Pd/UiO-66 were conducted by varying the stirring rates, from 500 rpm to 1200 rpm, while all other operating conditions were identical. As shown in Table S1, the impact of changing stirring rate on the FAL conversion and selectivity to the products are listed. Over different stirring rates, the FAL conversion were constant, while product selectivity changed slightly, suggesting that there is no obvious external diffusion control.

Subsequently, the reaction conditions such as catalyst dosage, reaction temperature and hydrogen pressure were optimized. FAL conversion was kept at 100%, and the selectivity to THFOL reached 100% when the catalyst dosage was larger than 0.05 g (Fig. S4). Increasing reaction temperature can increase product selectivity, achieving a 100% THFOL selectivity when reaction temperature was higher than 50 °C (Fig. 3a). Meantime, 100% selectivity of THFOL was obtained when the hydrogen pressure was increased to 1.0 MPa (Fig. 3b).

3.2.4. Catalyst recycling

To evaluate the stability of Pd/UiO-66 in aqueous phase FAL hydrogenation, the catalyst was reused for three times after separation of the catalyst by centrifugation. In the fourth run (Fig. S5), the selectivity to THFOL slightly decreased from 100% to 99%, indicating a slight decrease of the hydrogenation activity. The concentration of Pd species in the solution after the reaction was analyzed by ICP, the content of Pd was below the detection limit, ruling out the possibility of Pd metal leaching under the reaction conditions. In addition, the content of Pd in the solution was further determined by complexometric titration, and no Pd was titrated as well. In contrast, a tiny fraction of Zr (0.011 wt%) was detected by ICP analysis. Fig. S6 shows the XRD pattern of the spent Pd/UiO-66 catalyst after the four consecutive runs. Compared with the fresh catalyst, the decreased intensity of XRD peaks of the spent catalyst, suggesting there was slight loss in crystallinity, in agreement with the fraction of Zr leaching from the UiO-66 framework.

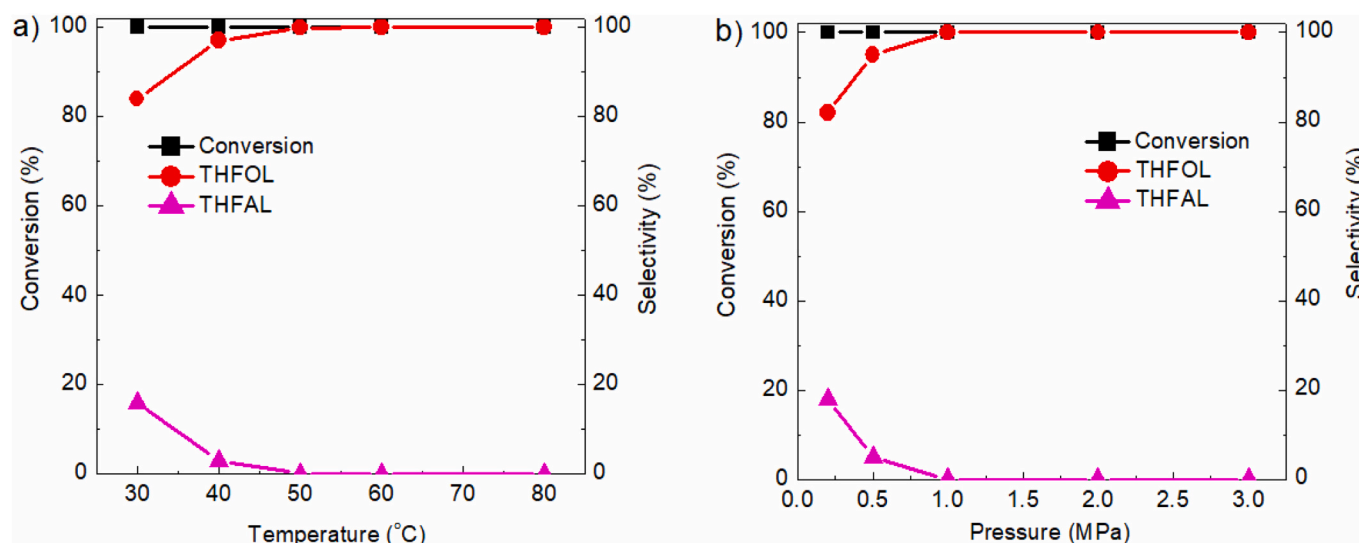


Fig. 3. a) Effect of reaction temperature on conversion and product selectivity in FAL hydrogenation catalyzed by Pd/Uio-66. b) Effect of hydrogen pressure on conversion and product selectivity in FAL hydrogenation catalyzed by Pd/Uio-66. Reaction conditions: 50 mg Pd/Uio-66 catalyst, 100 mg FAL, 9.9 g water, 4 h.

4. Conclusions

Water was found to be a preferable solvent for FAL hydrogenation catalyzed by Pd/Uio-66 to produce THFOL. Compared with Pd/ γ -Al₂O₃ and Pd/SiO₂, Pd/Uio-66 showed considerably higher catalytic performance in aqueous phase hydrogenation of FAL to THFOL. The enhanced performance of Pd/Uio-66 might be related with the high dispersion of Pd particles and the strong adsorption of FAL on Uio-66 in the gas-liquid-solid reaction. The aqueous phase hydrogenation of FAL to THFOL catalyzed by Pd/Uio-66 proceeded in two parallel pathways: (1) FAL was partially hydrogenated to FOL which was hydrogenated to THFOL; (2) FAL was partially hydrogenated to THFAL which was further hydrogenated to THFOL. It is found that the pathway of FAL-FOL-THFOL was much faster than the one of FAL-THFAL-THFOL, in which the hydrogenation of THFAL was rate-determining. Pd/Uio-66 did not show distinctive deactivation in four consecutive runs.

Declaration of Competing Interest

The authors declare that they have no known competing financial interests or personal relationships that could have appeared to influence the work reported in this paper.

Acknowledgements

This work was financially supported by International S&T Cooperation Program of China (2016YFE0109800), NSFC (21972014, 21603024, U1508205, 21473017, 21403025), the Fundamental Research Funds for the Central Universities (DUT19GJ205).

Appendix A. Supplementary data

Supplementary data to this article can be found online at <https://doi.org/10.1016/j.catcom.2020.106178>.

References

- [1] P. Gallezot, Conversion of biomass to selected chemical products, *Chem. Soc. Rev.* 41 (2012) 1538–1558.
- [2] S.P. Teong, G. Yi, Y. Zhang, Hydroxymethylfurfural production from bioresources: past, present and future, *Green Chem.* 16 (2014) 2015–2026.
- [3] K. Yan, G. Wu, T. Lafleur, C. Jarvis, Production, properties and catalytic hydrogenation of furfural to fuel additives and value-added chemicals, *Renew. Sust. Energ. Rev.* 38 (2014) 663–676.
- [4] Y. Nakagawa, K. Takada, M. Tamura, K. Tomishige, Total hydrogenation of furfural and 5-hydroxymethylfurfural over supported Pd–Ir alloy catalyst, *ACS Catal.* 4 (2014) 2718–2726.
- [5] B. Chen, F. Li, Z. Huang, G. Yuan, Tuning catalytic selectivity of liquid-phase hydrogenation of furfural via synergistic effects of supported bimetallic catalysts, *Appl. Catal. A Gen.* 500 (2015) 23–29.
- [6] S. Sitthitha, T. Sooknoi, Y. Ma, P.B. Balbuena, D.E. Resasco, Kinetics and mechanism of hydrogenation of furfural on Cu/SiO₂ catalysts, *J. Catal.* 277 (2011) 1–13.
- [7] N. Merat, C. Godawa, A. Gaset, J. Chem, High selective production of tetrahydrofurfuryl alcohol: catalytic hydrogenation of furfural and furfuryl alcohol, *Technol. Biotechnol.* 48 (1990) 145–159.
- [8] N.S. Biradar, A.A. Hengne, S.N. Birajdar, R. Swami, C.V. Rode, Tailoring the product distribution with batch and continuous process options in catalytic hydrogenation of furfural, *Org. Process. Res. Dev.* 18 (2014) 1434–1442.
- [9] S. Bhogswararao, D. Srinivas, Catalytic conversion of furfural to industrial chemicals over supported Pt and Pd catalysts, *J. Catal.* 327 (2015) 65–77.
- [10] C. Li, G. Xu, X. Liu, Y. Zhang, Y. Fu, Hydrogenation of biomass-derived furfural to tetrahydrofurfuryl alcohol over hydroxyapatite-supported Pd catalyst under mild conditions, *Ind. Eng. Chem. Res.* 56 (2017) 8843–8849.
- [11] D. Yin, H. Ren, C. Li, J. Liu, C. Liang, Highly selective hydrogenation of furfural to tetrahydrofurfuryl alcohol over MIL-101(Cr)-NH₂ supported Pd catalyst at low temperature, *Chin. J. Catal.* 39 (2018) 319–326.
- [12] M. Hronec, K. Fulajtarová, Selective transformation of furfural to cyclopentanone, *Catal. Commun.* 24 (2012) 100–104.
- [13] V.V. Ordonsky, J.C. Schouten, J.V. Schaaf, T.A. Nijhuis, Biphasic single-reactor process for dehydration of xylose and hydrogenation of produced furfural, *Appl. Catal. A Gen.* 451 (2013) 6–13.
- [14] A.B. Merlo, V. Vetere, J.F. Ruggera, M.L. Casella, Bimetallic PtSn catalyst for the selective hydrogenation of furfural to furfuryl alcohol in liquid-phase, *Catal. Commun.* 10 (2009) 1665–1669.
- [15] R. Fang, L. Chen, Z. Shen, Y. Li, Efficient hydrogenation of furfural to furfuryl alcohol over hierarchical MOF immobilized metal catalysts, *Catal. Today* (2020), <https://doi.org/10.1016/j.cattod.2020.03.019>.
- [16] Y. Wang, C. Liu, X. Zhang, One-step encapsulation of bimetallic Pd–Co nanoparticles within Uio-66 for selective conversion of furfural to cyclopentanone, *Catal. Lett.* 150 (2020) 2158–2166.
- [17] A. Corma, H. García, F.X.L.S. Xamena, Engineering metal organic frameworks for heterogeneous catalysis, *Chem. Rev.* 110 (2010) 4606–4655.
- [18] J.H. Cavka, S. Jakobsen, U. Olsbye, N. Guillou, C. Lamberti, S. Bordiga, K.P. Lillerud, A new zirconium inorganic building brick forming metal organic frameworks with exceptional stability, *J. Am. Chem. Soc.* 130 (2008) 13850–13851.
- [19] Y. Yang, D. Deng, D. Sui, Y. Xie, D. Li, Y. Duan, Facile preparation of Pd/Uio-66-v for the conversion of furfuryl alcohol to tetrahydrofurfuryl alcohol under mild conditions in water, *Nanomaterials* 9 (2019) 1698.
- [20] J. Freel, Chemisorption on supported platinum: I. evaluation of a pulse method, *J. Catal.* 25 (1972) 139–148.
- [21] M.A. Aramendía, V. Borau, C. Jiménez, J.M. Marinas, A. Moreno, Comparative measurements of the dispersion of Pd catalyst on SiO₂-AlPO₄ support using TEM and H₂ chemisorption, *Colloids Surf. A Physicochem. Eng. Asp.* 106 (1996) 161–165.
- [22] J. Ren, A. Wang, X. Li, Y. Chen, H. Liu, Y. Hu, Hydrodesulfurization of dibenzothiophene catalyzed by Ni–Mo sulfides supported on a mixture of MCM-41 and HY zeolite, *Appl. Catal. A Gen.* 344 (2008) 175–182.
- [23] V.N. Panchenko, M.M. Matrosova, J. Jeon, J.W. Jun, M.N. Timofeeva, S.H. Jung, Catalytic behavior of metal-organic frameworks in the Knoevenagel condensation

- reaction, *J. Catal.* 316 (2014) 251–259.
- [24] S.H. Pang, C.A. Schoenbaum, D.K. Schwartz, J.W. Medlin, Effects of thiol modifiers on the kinetics of furfural hydrogenation over Pd catalysts, *ACS Catal.* 4 (2014) 3123–3131.
- [25] Á. O'Driscoll, J.J. Leahy, T. Curtin, The influence of metal selection on catalyst activity for the liquid phase hydrogenation of furfural to furfuryl alcohol, *Catal. Today* 279 (2017) 194–201.
- [26] X. Hu, S. Kadarwati, Y. Song, C. Li, Simultaneous hydrogenation and acid-catalyzed conversion of the biomass-derived furans in solvents with distinct polarities, *RSC Adv.* 6 (2016) 4647–4656.
- [27] M. Behrens, G. Lolli, N. Muratova, I. Kasatkin, M. Hävecker, R.N. D'Alnoncourt, O. Storcheva, K. Köhler, M. Muhler, R. Schlögl, The effect of Al-doping on ZnO nanoparticles applied as catalyst support, *Phys. Chem. Chem. Phys.* 15 (2013) 1374–1381.
- [28] M.J. Taylor, L.J. Dumdel, M.A. Isaacs, C.M.A. Parlett, K. Wilson, A.F. Lee, G. Kyriakou, Highly selective hydrogenation of furfural over supported Pt nanoparticles under mild conditions, *Appl. Catal. B Environ.* 180 (2016) 580–585.
- [29] Z. Zhao, R. Bababrik, W. Xue, Y. Li, N.M. Briggs, D. Nguyen, U. Nguyen, S.P. Crossley, S. Wang, B. Wang, D.E. Resasco, Solvent-mediated charge separation drives alternative hydrogenation path of furanics in liquid water, *Nat. Catal.* 2 (2019) 431–436.
- [30] H. Wan, A. Vitter, R.V. Chaudhari, B. Subramaniam, Kinetic investigations of unusual solvent effects during Ru/C catalyzed hydrogenation of model oxygenates, *J. Catal.* 309 (2014) 174–184.
- [31] R.M. Mironenko, V.P. Talsi, T.I. Gulyaeva, M.V. Trenikhin, O.B. Belskaya, Aqueous-phase hydrogenation of furfural over supported palladium catalysts: effect of the support on the reaction routes, *React. Kinet. Mech. Catal.* 126 (2019) 811–827.
- [32] R. Fang, H. Liu, R. Luque, Y. Li, Efficient and selective hydrogenation of biomass-derived furfural to cyclopentanone using Ru catalysts, *Green Chem.* 17 (2015) 4183–4188.
- [33] M. Zhao, K. Yuan, Y. Wang, G. Li, J. Guo, L. Gu, W. Hu, H. Zhao, Z. Tang, Metal-organic frameworks as selectivity regulators for hydrogenation reactions, *Nature* 539 (2016) 76–80.
- [34] D. Jiang, G. Fang, Y. Tong, X. Wu, Y. Wang, D. Hong, W. Leng, Z. Liang, P. Tu, L. Liu, K. Xu, J. Ni, X. Li, Multifunctional Pd@UiO-66 catalysts for continuous catalytic upgrading of ethanol to n-butanol, *ACS Catal.* 8 (2018) 11973–11978.
- [35] R. Krishna, C. Ramakrishna, K. Soni, T. Gopi, G. Swetha, B. Saini, S.C. Shekar, Effect of alkali carbonate/bicarbonate on citral hydrogenation over Pd/carbon molecular sieves catalysts in aqueous media, *Mod. Res. Catal.* 05 (2016) 1–10.